PERGAMON

International Journal of Multiphase Flow 25 (1999) 1181–1194

International Journal of Multiphase Flow

www.elsevier.com/locate/ijmulflow

Phase distribution and bubble velocity in two-phase slit flow

St. Körner, L. Friedel*

Techn. Univ. Hamburg-Harburg, D-21071 Hamburg, Germany

Received 10 November 1998; received in revised form 1 June 1999

Dedicated to Gad Hetsroni on the occasion of his 65th birthday and in honour of his always friendly guidance into the complex field of two-phase flow full of well and ill posed problems as well as sometimes spurious analytical solutions.

Abstract

The phase distribution, the bubble velocities and the thermal expansion behaviour of the bubbles in two-phase bubbly slit flow were examined by using high-speed cinematography. The phase distribution in (adiabatic) flashing water and non flashing air/water flow is relatively homogeneous. Under all flow conditions the slip ratio in the one dimensional flow is less than 1.2. It can be recalculated by assuming the pressure and the friction forces on the bubble surface in equilibrium. The cavitation in a slightly subcooled liquid occurring at a sharp edged slit inlet has a significant influence on the post-evaporation behaviour. In principle, the assumption of a homogeneous mixture flow in thermodynamic equilibrium is validated, the deviations are mutually neutralizing to a large extent.

Keywords: Two-phase flow; Slit flow; Phase distribution; Bubble velocity flashing water; Air/water

1. Status and problem

According to the literature given on two-phase leak flow models, e.g., Abdollahian and Chexal (1983), Amos and Schrock (1983), Chexal et al. (1984), Jones (1976), Leung and Grolmes (1987), Schrock et al. (1986) the prediction of the two-phase mass flux for a given pressure difference requires knowledge of the boiling delay or of the thermodynamic non-

* Corresponding author.

0301-9322/99/$ - see front matter
PII: S0301-9322(99)00055-5

equilibrium between the phases but also of the magnitude of the mean fluid dynamic non-equilibrium in form of the slip. Referring to John et al. (1988), Westphal (1991) or Westphal and Friedel (1992) the highest predictive accuracy for the two-phase mass flow through so-called subcritical wall cracks, resp. narrow rectangular slits is obtained by using the Homogeneous Equilibrium Model according to Pana (1975). Its use is well established in the (German) nuclear power industry and no other more complete and better validated mass flow model has been published since (Körner, 1999). This model includes the assumption of homogeneous flow, respectively a negligibly small slip, an immediate adjustment of the thermodynamic equilibrium between the phases on the basis of the actual saturation pressure and a friction pressure drop submodel. The overall suitability of the model by Pana (1975) seems not to be logical, since in accordance with the common experience with the (isentropic) homogeneous equilibrium model (in comparison to other mass flow models) the minimum (critical) mass flux is predicted for given equal stagnation conditions. Taking intentionally a boiling delay and/or heterogeneous flow into account, a significantly larger mass flux is predicted. In view of the fact that each submodel includes assumptions which in reality may not be fully met, it cannot be reasonably excluded that the appropriate prediction of the two-phase mass flux is caused only by the mutual compensation of simplifying assumptions or incompletenesses in the submodels. Hence, the extrapolatability of the model by Pana (1975) can not be taken for granted. To ensure further the technical use of this model the assumptions introduced were validated separately in this work.

2. Aim and approach

For separate validation of the assumption concerning the ignored slip, dedicated experiments were conducted. Using high-speed cinematography with a picture frequency of up to 20 kHz the phase distributions in flashing water and unheated air/water bubbly flow have been recorded. After processing the results by object-detection algorithms and computer based picture analysis, the velocities of the bubbles are obtained. The details about the instrumentation, e.g., the high-speed system used and the data analysis, as well as the range of experimental conditions are given by Körner and Friedel (1998a). The velocities have been compared to the calculated ones on the basis of a homogeneous mixture. Additionally, the state change of the air in the bubbles was estimated on the basis of the volume increase due to the pressure decrease along the flow path.

3. Narrow slit test section

In the experiments, an adiabatic model slit in the form of a channel with a constant rectangular cross section limited by two borosilicate glass or plexiglass walls was used, so that the movement of the bubbles could be observed optically along the total flow path (Fig. 1). In the larger cross section upstream of the test section the mean velocity is negligibly small compared to that in the slit. Therefore, the recorded wall pressure practically equals with the stagnation pressure and thermodynamic equilibrium, respectively, the same temperature for

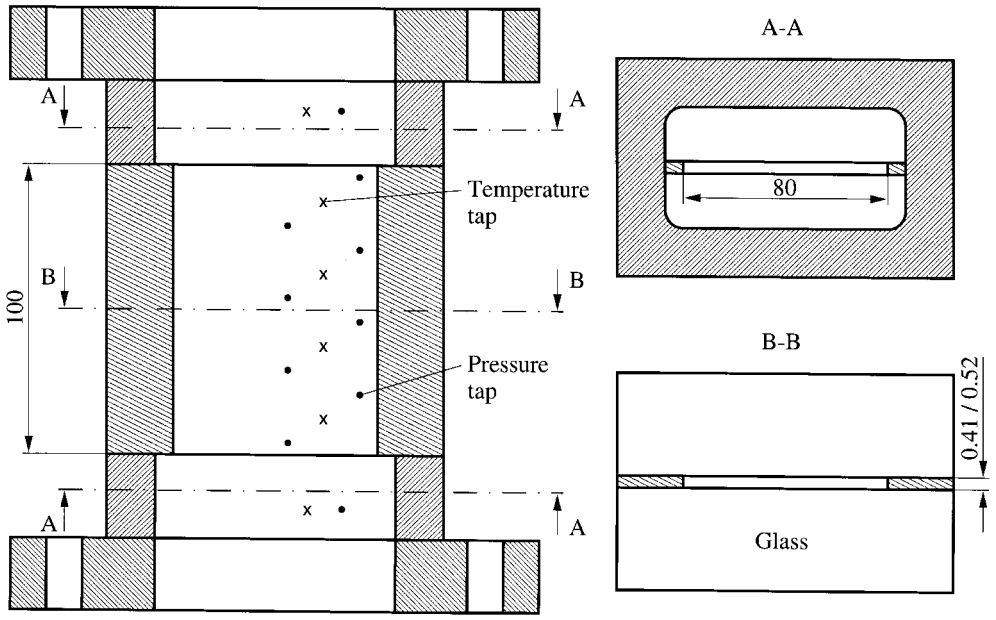

Fig. 1. Geometrical dimensions of the model slit and arrangement of the pressure and temperature taps.

both nearly stagnant phases can be presumed. The value of the test section aspect ratio amounts to more than 100. As a consequence of the small channel opening, in the range of some 0.5 mm, the pressure loss due to friction (and momentum exchange between the phases) should mainly contribute to the total pressure drop in relation to that due to acceleration and the negligibly small geodetical lift. Accordingly, the gravity force exhibits no significant influence on the flow pattern and on the pressure drop, but it promotes the tendency for the phases to separate in the low speed flow region upstream of the test section. With respect to the experimental procedure, in order to avoid a phase inversion in the bubbly flow regime, the air/water experiments were conducted with upward flow. On the contrary, with flashing water flow the (subcooled) liquid-phase could only be discharged from the bottom of the test vessel, so the experiments had to be carried out with downward flow.

4. Phase distribution in water/air bubbly flow

The bubbles in the flow seem to be relatively homogeneously distributed across the flow cross section (Fig. 2). The equivalent diameter of the bubbles varies in a wide range even at the same longitudinal position in the slit, the bubble volumes being between 0.5 and some 100 mm^3. An effect of the static device used for mixing the air and the water on the distribution and the size of the bubbles could not be observed. This may be attributable to the distance of more than 200 hydraulic diameters between the mixer and the slit inlet and especially to the negligibly small velocity of the mixture upstream of the slit. Both features induce a relatively

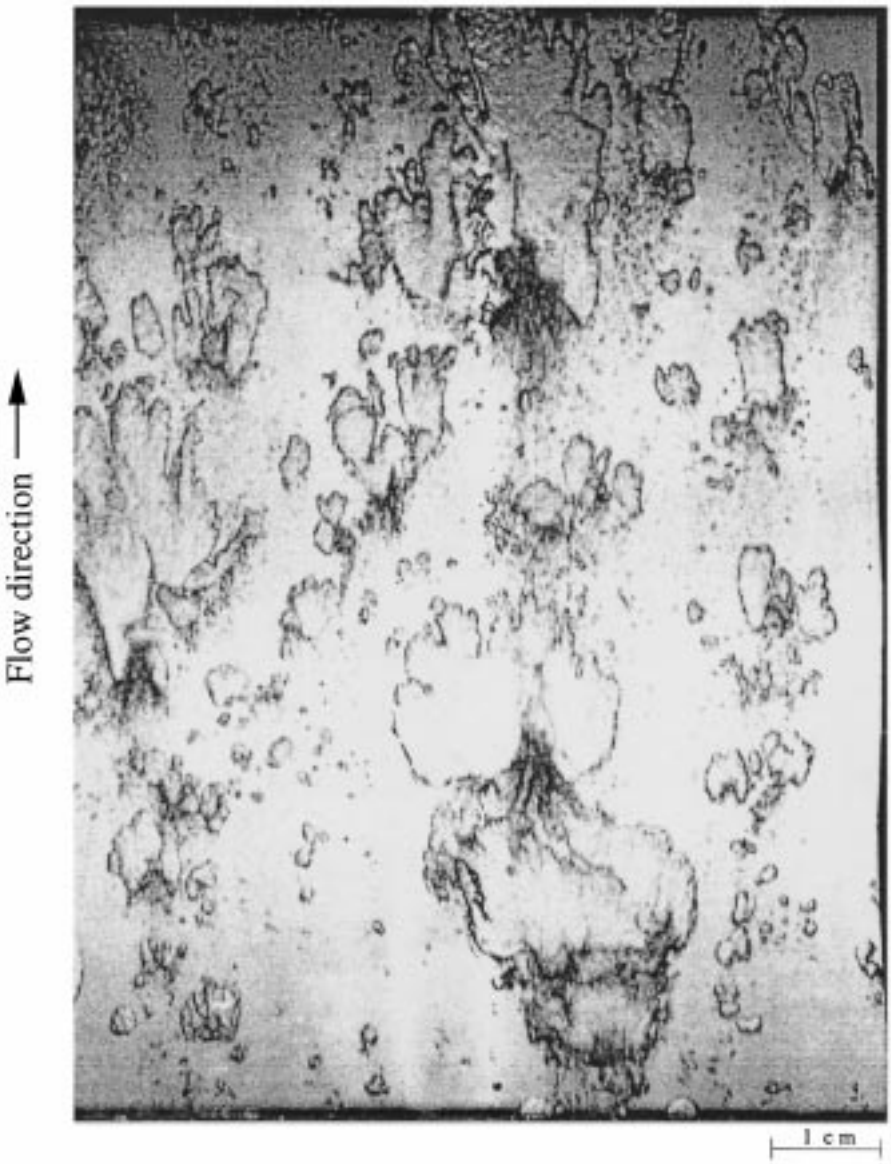

Fig. 2. Photography of a vertical upward (unheated) air/water slit flow (opening 0.52 mm, length 100 mm) for a pressure difference of 4 bar and mass flow quality of 0.1%.

long total mean residence time of the bubbles in the pipe before entering the slit allowing, thus, for a self-established bubble population.

In the test section the (specific) air volume increases, mainly because of the pressure decay due to friction along the flow path. As a consequence, the individual bubbles expand and the corresponding water volume has to be displaced. As a result of the relatively steep local pressure gradient in the downstream flow direction and the lesser effort required for removal of the concurrently flowing water, the bubbles expand mainly at the top, herewith forming streaks

and indentations. The reason for this behaviour can be seen in local random interactions, respectively metastable equilibria, between the forces in the bubble top surface and those due to the turbulence and the inertia of the surrounding water. This effect is especially observed for large diameter air bubbles. In this case, due to the great radius of curvature the surface forces exhibit only a relatively small impact on the resulting structure of the interface. The consequence is an irregular and fissured, large specific surface area of the bubbles at the top.

5. Phase distribution in flashing water flow

Considering subcooled water flow at the inlet of the adiabatic slit, the falling pressure (due to pressure drop) can attain the saturation pressure corresponding to the mean local fluid temperature further downstream, or even fall below. In the latter case, the water in the slit becomes superheated and finally flashing sets in (Fig. 3). In this experiment, a pressure distribution along the downward flow path is established in such a way that at a distance of some 20 mm upstream of the slit outlet the saturation pressure is just reached. Regarding the actual boiling inception in technically pure or clean superheated liquids, flashing can only start on the surface of existing activable nuclei. These are normally present as small bubbles or microbubbles adsorbed on crevices in the walls of the channel, respectively, on impurities in the water. Because of these nuclei small (spherical) steam bubbles form — averaged over the time — rather homogeneously distributed in the superheated water.[1] With further decrease of the pressure along the flow path, the bubbles expand while in parallel, as a consequence of the progressing phase change due to flashing, their volumes steadily increase. Herewith, due to the necessary large nucleus formation energy, the number of bubbles remain nearly constant. Despite of the remarkable volume increase, the radii of the steam bubbles are here considerably smaller and remain within a narrower diameter range than those of the formerly shown air bubbles for quasi identical density ratios. This can be attributed to the different origin or generation of the air, respectively, steam bubbles in the surrounding water.

For an initially subcooled water inlet flow at a larger mass flow rate, as a consequence of the abrupt decrease in the cross section at the slit inlet and vortex generation or flow detachment, bubbles can develop due to cavitation caused by a local pressure undershoot in the vena contracta (Isay, 1989), see Fig. 4. To emphasize this effect the slit inlet was modified by installing a sharp edged short orifice with a diameter of about 50% of the slit width shortly ahead of the test section. Thus, in this special case, an inlet velocity distribution is enforced with a remarkably higher fluid velocity in the center than at the periphery of the slit inlet. As a consequence of the smaller local velocity and, therefore, the modest pressure change at the periphery, no cavitation bubbles could be created or they are (at least) invisible in the photography. Downstream of the slit inlet, the center flow is strongly decelerated due to the re-attachment at the wall and the establishment of a fully developed velocity profile. Correspondingly, the local pressure increases

[1] Because of the smooth surface of the borosilicate glass walls, the boiling nuclei are here mainly adsorbed on impurities supposed to be rather homogeneously distributed in the flowing liquid. The uneven distribution of the bubbles can be attributed to the random nucleation process, in this special recording instant, predominantly at the right side of the slit.

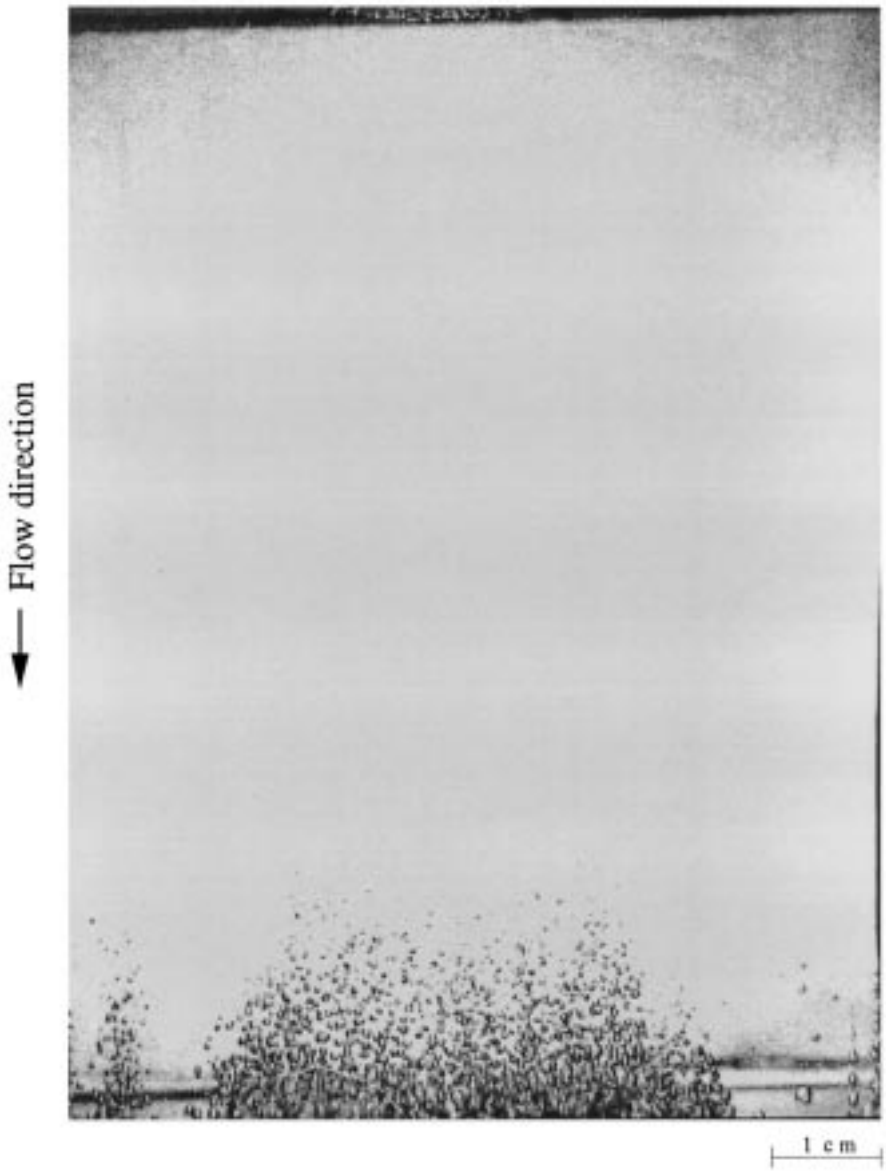

Fig. 3. Photography of vertical downward (adiabatic) flashing water slit flow (opening 0.41 mm, length 100 mm) for inlet stagnation pressure of 1.3 bar and initial subcooling of 3 K.

and the cavitation bubbles collapse. However, a substantially large number of microbubbles consisting of non or only slowly condensable gases are supposed to remain in water. Because of their tiny diameter in the range of just 1 μm these bubbles are hard to detect (Westphal, 1981) and are almost invisible in the photography shown. If further downstream the saturation pressure of the water is again significantly undershot, compared to that in the still partly undisturbed water at the periphery, a larger number of microbubbles can immediately be reactivated to act as

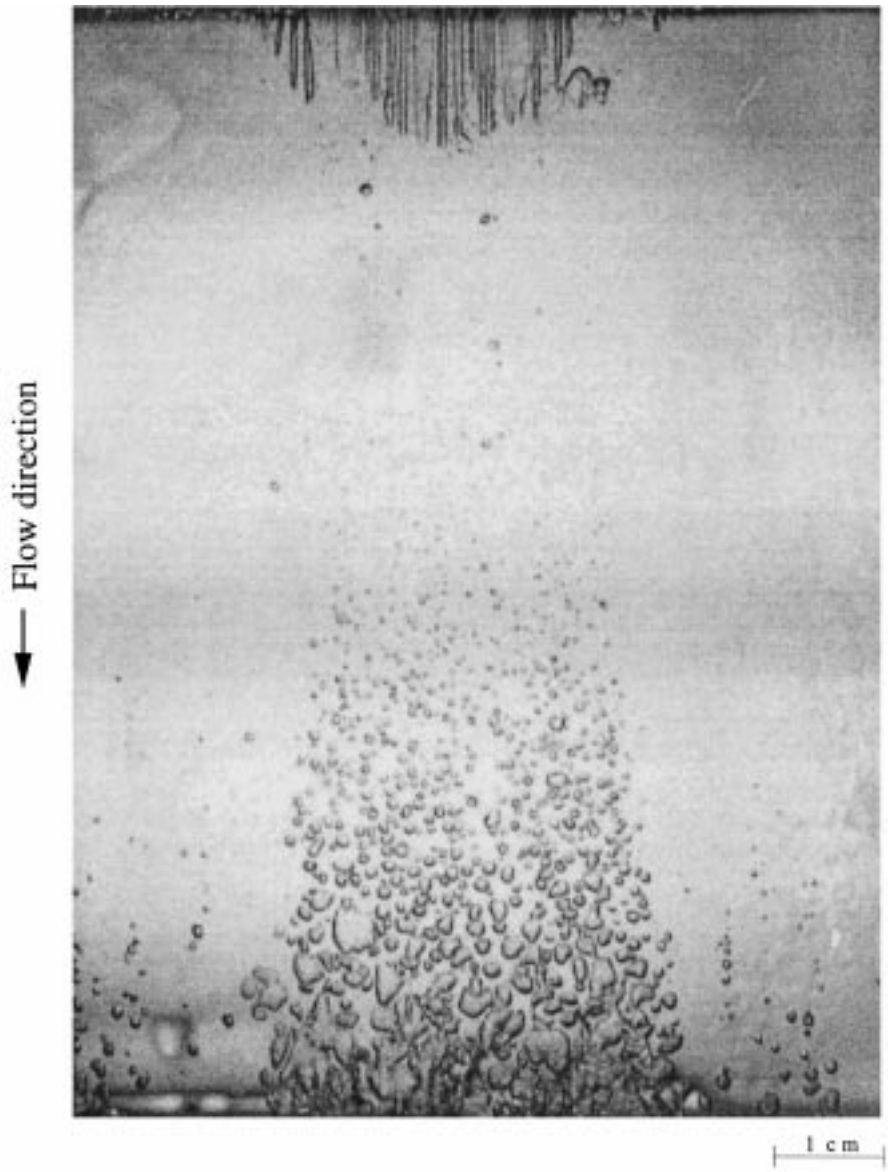

Fig. 4. Photography of vertical downward (adiabatic) flashing water slit flow (opening 0.41 mm, length 100 mm) coupled with an inlet orifice imposing a modified velocity profile. Inlet stagnation pressure of 5 bar and initial subcooling of 5 K.

boiling nuclei for initiation of phase change. Consequently, now more intensive flashing occurs and a quasi homogeneous bubble distribution in the flashing water jet is attained. Besides this, the higher fluid velocity causes more intensive turbulence and, thus, a larger heat flux from the superheated water to the bubble surface, so that the boiling delay is less significant. In conclusion, it is obvious that in case of cavitation bubbles created at a sharp edged inlet, a smaller water superheat develops despite of the higher mean velocity.

In case of initially nearly saturated inlet water flow and high mean velocities (typical of fluiddynamic critical flow) the cavitation bubbles induced at the inlet do not collapse or vanish totally at the slit outlet when the time for the condensation is too short or the initial subcooling is too small. On the contrary, a considerable part of the bubbles remain, till the saturation pressure is again undershot and then act as nuclei so that intensive and early flashing occurs (Fig. 5). As a consequence of the new enlarged interphase area and enhanced evaporation, only a negligibly small water superheat can be established and the local pressure

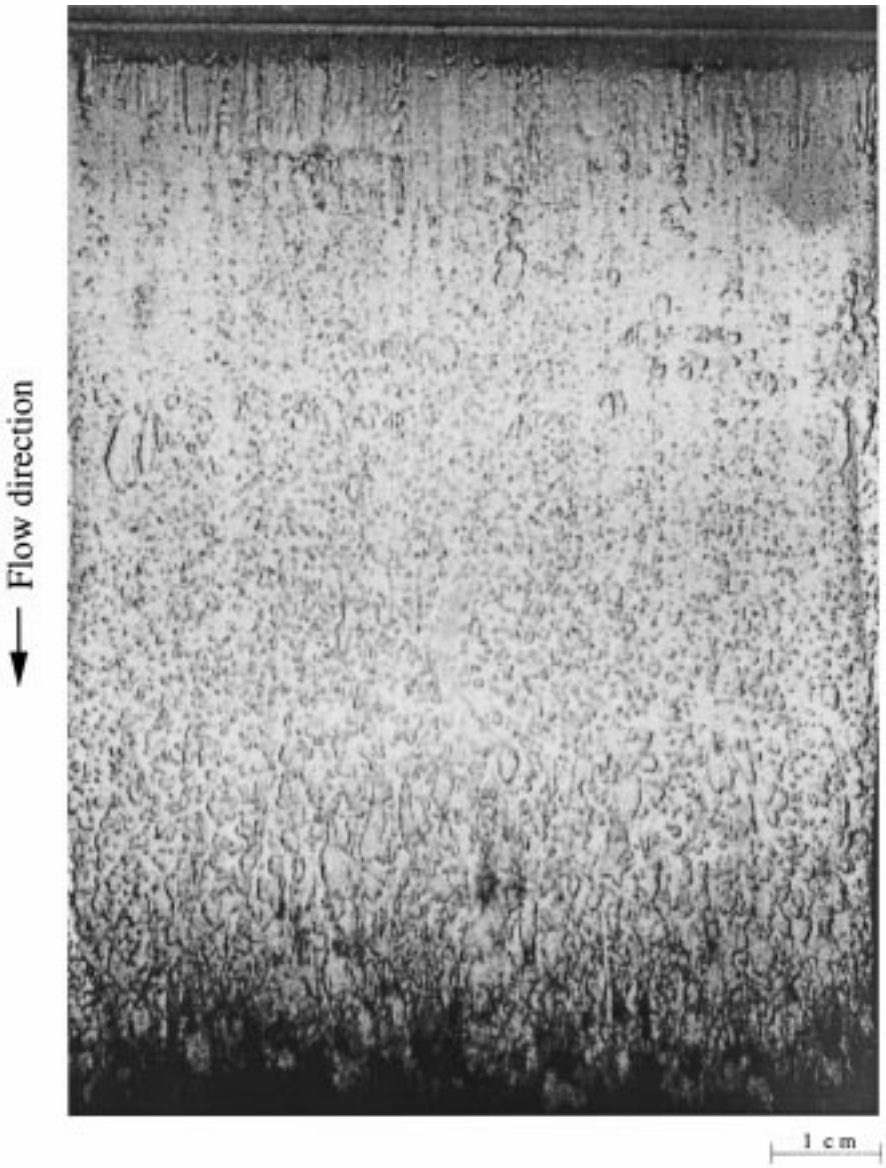

Fig. 5. Photography of vertical downward (adiabatic) flashing water slit flow (opening 0.41 mm, length 100 mm) for an inlet stagnation pressure of 12 bar and initial subcooling of 1 K.

and temperature of the mixture along the flow path are in reasonable agreement with the static equilibrium values (Körner and Friedel, 1998b). Again, caused by the decreasing pressure and the evaporation, the bubble volume increases. But, though physico-chemical coalescence or mechanical disproportioning of neighbouring bubbles may have occurred, again the recorded diameters are significantly smaller and within a narrower diameter band than those observed in air/water bubbly flow in the nearly same range of density ratio. The bubble sizes are also more homogeneously distributed in the transversal direction.

6. Change of state of the air in the bubbles

For a relatively large bubble with an air mass of 0.3 mg, the change of the volume along the slit length in contrast to that at the inlet was compared to the calculated volume increase assuming an isothermal and an adiabatic expansion, respectively (Fig. 6). Obviously, the experimental results at the slit inlet are closer to the lower curve based on an adiabatic change of state. With increasing distance, respectively residence time of the bubbles in the channel, a more isothermal expansion behaviour is approached. For distances greater than about 50 mm downstream of the inlet, a significant deviation between the experimental results and the calculated curve assuming isothermal change of state can no longer be observed. Indeed, the latter isothermal behaviour seems logical as the temperature decrease induced by the pressure profile along the flow path is slow compared to the (rapid) change at the sharp edged inlet.

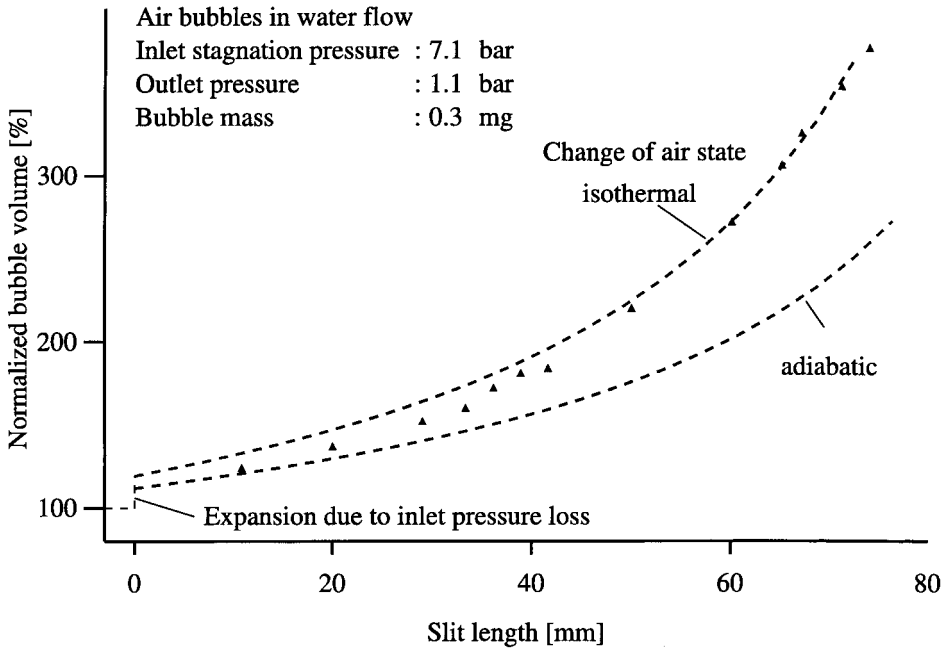

Fig. 6. Experimental normalized bubble volume and predictions assuming isothermal and adiabatic change of state of the air in the bubble, as a function of the slit length.

With respect to the air streaks developed during the bubble (top) expansion, the relatively large specific interphase contact area allows for a high specific heat flux and, thus, a small resulting temperature difference between the phases will get established. Applying this idea to the behaviour of smaller bubbles in flashing flow, due to their higher specific surface area and their lesser heat capacity, thermal equilibrium will be attained earlier, so that isothermal behaviour can be attributed with a higher degree of reasonableness.

7. Bubble velocity and slip

The measured local (absolute) velocities of the bubbles in (unheated, non-flashing) air/water flow with a mass flow quality of 0.05% are depicted in Fig. 7. Bubbles with a volume between 3 and approx. 40 mm^3 are encountered in transversal as well as in the longitudinal direction. As the bubble volume is getting larger a degressive increase of the measured velocity is evident. This trend is well known from the literature for a single bubble rising in stagnant water, and should also be true at least for upward flowing two-phase mixtures. In this context, the relatively higher velocities of the larger bubbles can be related to the smaller specific interphase area. As a result, less intensive momentum exchange between the phases occurs. Depending on the position in the slit, the (static) pressure decreases significantly between the inlet and the outlet. As a consequence, the air density and the calculated homogeneous mixture density

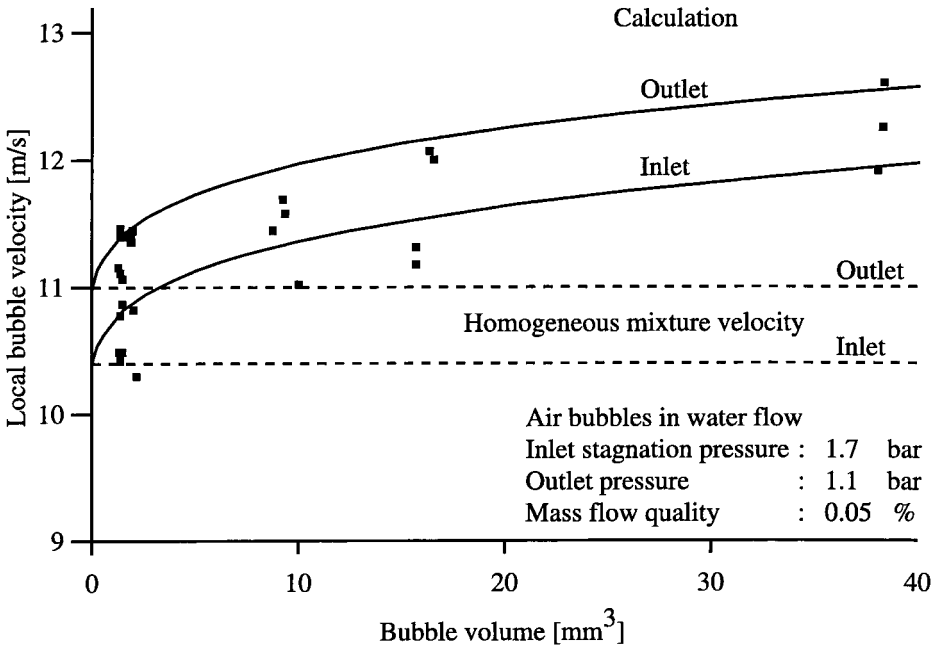

Fig. 7. Calculated and measured local air bubble velocities in vertical upward (unheated) air/water flow (opening 1.1 mm, length 100 mm) as a function of the bubble, volume. Inlet stagnation pressure of 1.7 bar, outlet pressure of 1.1 bar and mass flow quality of 0.05%.

decrease. In this environment, the large variation of the absolute bubble velocity on an equal volume basis, is coupled with the local position in the slit at the instant of recording, the lower values corresponding to the inlet position with the smaller liquid velocity. At the outlet, due to the inferior pressure, larger velocities prevail. This trend is also reflected in the calculated homogeneous mixture velocity, the velocities being here between some 10.4 and 11 m/s. An additional variation in the measurements is introduced by the irregular top side expansion of the bubbles, the interactions between their movement in a swarm and the turbulence forces in the surrounding water flow. Indeed, only the mean value of the velocities of small bubbles would be quite close to that calculated assuming one-dimensional homogeneous flow. For larger bubbles, nevertheless, significant deviations between the actual velocity and that of the homogeneous mixture are evident, even at the same longitudinal position in the slit.

On the basis of the (measured) individual mass fluxes, the local pressure, respectively the air and water densities, as well as the mean bubble velocity, the mean water velocity and the (local) slip ratio can be calculated at a given longitudinal and transversal position in the slit. It is evident from Fig. 8 that, in parallel to the trend seen for the bubble velocity, the slip ratio also increases with larger bubble volumes and with bubble position in the slit and is largest at the outlet. For the smallest bubble size, the derived mean slip ratio is nearly unity. Even for the largest bubbles the maximum experimental (local) slip ratio is less than 1.2, allowing in a first approximation application of the homogeneous mixture flow assumption in the transversal and longitudinal directions.

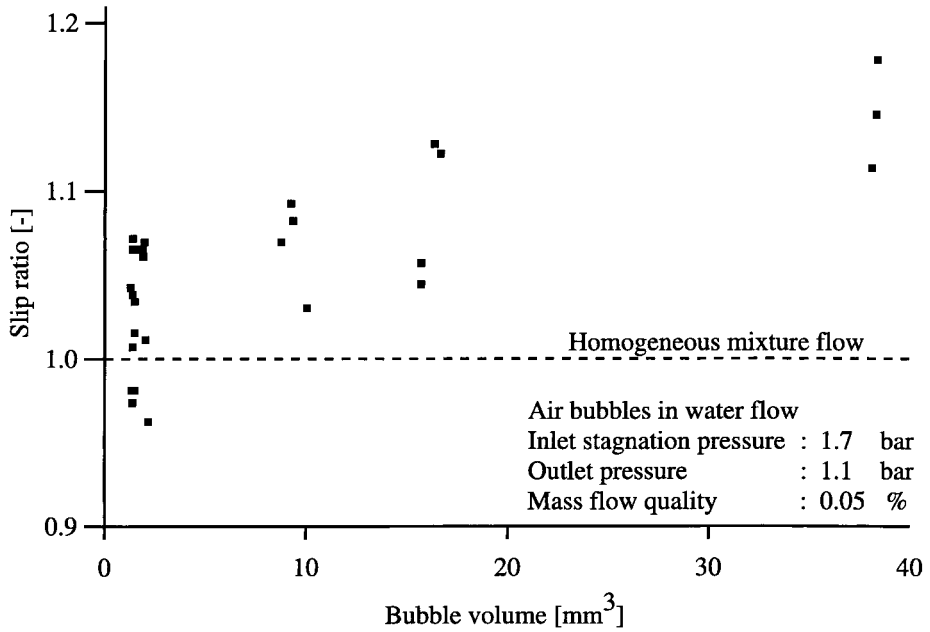

Fig. 8. Calculated local slip ratio in vertical upward (unheated) air/water slit flow (opening 1.1 mm, length 100 mm) as a function of the bubble volume. Inlet stagnation pressure of 1.7 bar, outlet pressure of 1.1 bar and mass flow quality of 0.05%.

8. Recalculation of the bubble velocity

The final velocity of a single air bubble in stationary water flow can be estimated by using the (static) equilibrium between the driving pressure force, buoyancy and the resistance force due to friction.

The pressure force

$$F_{\Delta p} = \int_O p \, \mathrm{d}O_{\mathrm{Bubble}} \tag{1}$$

follows from integrating the local pressure distribution p on the bubble surface O_{Bubble}.

Assuming a single spherical gas bubble, following Bird et al. (1960) the resistance force can be calculated using the drag coefficient for bubbles according to

$$F_{\mathrm{R}} = c_{\mathrm{W}} \frac{\pi}{4} D_{\mathrm{Bubble}}^2 \frac{\rho_{\mathrm{liq}}}{2} \left(\bar{u}_{\mathrm{Bubble}}^2 - \bar{u}_{\mathrm{liq}}^2 \right) \tag{2}$$

with

$$c_{\mathrm{W}} = \frac{21}{Re} + \frac{6}{\sqrt{Re}} + 0.28$$

for

$$Re = \frac{D_{\mathrm{Bubble}} \left(\bar{u}_{\mathrm{Bubble}} - \bar{u}_{\mathrm{liq}} \right)}{\nu_{\mathrm{liq}}} \leq 4000 \tag{3}$$

where symbols have their usual meaning.

The stationary, single bubble velocity in the liquid, after rearrangement, results from

$$\bar{u}_{\mathrm{Bubble}} = \sqrt{\bar{u}_{\mathrm{liq}}^2 + \frac{\rho_{\mathrm{liq}} - \rho_{\mathrm{g}}}{\rho_{\mathrm{liq}}^2} \frac{8}{c_{\mathrm{W}} \pi D_{\mathrm{Bubble}}^2} \int_O p \, \mathrm{d}O_{\mathrm{Bubble}}} \tag{4}$$

For a given bubble diameter and pressure profile along the flow path, which can be calculated, e.g., by integrating the Bernoulli equation for compressible fluids (at subcritical flow conditions) after introducing a dissipative term,[2] the drift velocity of the bubbles depending on their size can be estimated (Körner, 1999). It is herewith assumed that the interactions, respectively the momentum exchange between the bubbles, are negligibly small compared to that with the surrounding water, as the mean liquid-phase velocity exceeds by far the free ascending bubble velocity.

The predicted bubble velocities in air/water flow along with the former already quoted experimental data are given in Fig. 7. As the pressure decays and the water velocity increases along the slit length, the bubble velocities for different sizes are calculated for the inlet and the

[2] The geodetical pressure change is negligibly small in comparison to the terms considering dissipation and momentum change.

outlet conditions. Again with the assumption of a negligibly small momentum exchange between the bubbles compared to that between the phases, in principle, all experimental values should be found between these two limiting graphs. For larger bubble volumes this is true, whereas some of the smaller bubbles are actually slower than predicted. This deviation could be nevertheless referred to interactions between the movement of the bubbles in a swarm and the (turbulent) water flow, the deceleration of the liquid flow caused by the higher velocity of large bubbles as well as especially to the incompleteness of the one-dimensional mixture flow assumptions.

The mass flow quality in flashing two-phase flow cannot yet be accurately predicted due to the occurrence of a non measurable boiling delay. As a consequence, an unambiguous slip velocity is not calculable from the measured bubble velocities. In view of the fact that a statement about the steam bubble drift velocity would be helpful, the thesis is offered that the (measured) drift velocities in air/water flow should not significantly differ from those in flashing water flow for an equal bubble diameter range, an identical local pressure gradient and a similar density ratio. This thesis is based on the evidence that, in comparison to the bubble sizes in air/water mixtures, the bubbles in flashing water flow are in a more narrow diameter band and smaller and, therefore, more spherical. This property would already allow for a more uniform radial expansion and lower bubble drift velocities and, therefore, a proper representation of the homogeneous mixture flow assumption. Further on, in view of the quasi identical thermodynamic (boiling) conditions for all nuclei at a certain longitudinal position in the slit, the size of the steam bubbles at the same distance downstream of the inlet are (again) in the same range. Therefore, also due to this the velocities should not significantly differ against each other, especially when compared to the variations prevailing in air/water bubbly flow. In view of all these arguments a quasi homogeneous mixture flow assumption seems even more reasonable.

9. Experimental error

The reported experimental results represent time averaged mean values due to the inevitable chaotic behaviour of the two phases, even under well controlled stationary flow conditions in a laboratory environment. The experimental error is assessed to be some 8% (Körner and Friedel, 1998a) and, thus, is found in the usual scatter range of such experimental results.

10. Conclusion

The phase distribution in (adiabatic) flashing water and (unheated) air/water bubbly flow is relatively homogeneous. Significant differences, especially with respect to the transversal bubble size distribution and the structure of the interphase area, however, are observed. Due to the pressure undershoot in the sharp edged slit inlet, cavitation bubbles can be formed even in slightly subcooled water. Consequently, a larger number of microbubbles can be activated for initiation of flashing in the slit resulting in this case in a significantly smaller liquid superheat.

Apart from the local adiabatic expansion of the air in the bubble in an air/water flow caused

by the rapid pressure decrease at the slit inlet, further downstream an almost isothermal expansion is occurring. The mean velocity of the bubble does not significantly differ from that of the homogeneous mixture, it only slightly increases with higher bubble volume. The local slip ratio is in all cases less than 1.2 for the largest bubbles, so a quasi homogeneous one-dimensional two-phase flow can be assumed. The isothermal expansion at the later stage and the identity between the homogeneous mixture velocity and that of the bubbles may be referred to the high specific interphase area caused by the irregular bubble top expansion and resulting air streaks. The stationary drift velocity of the air bubbles can be recalculated based on the equilibrium between the pressure and the friction forces on the bubble surface. In principle, the assumption of homogeneous mixture flow in thermodynamic equilibrium in the slit used by Pana (1975) is acceptable for technical purposes.

References

Abdollahian, D., Chexal, B., 1983. Calculation of leak rates through cracks in pipes and tubes. EPRI Report NP-3395.

Amos, C.N., Schrock, V.E., 1983. Critical discharge of initially subcooled water through slits. Report NUREG/CR-3475, LBL-16363.

Bird, R.B., Stewart, W.E., Lightfood, E.N., 1960. Transport Phenomena. Wiley, New York.

Chexal, B., Abdollahian, D., Norris, D., 1984. Analytical prediction of single phase and two-phase flow through cracks in pipes and tubes. AIChE Symp. Series Heat Transfer 236 (80), 19–23.

Isay, W.-H., 1989. Kavitation. Schiffahrts-Verlag, Hansa, Hamburg.

John, H., Reimann, J., Westphal, F., Friedel, L., 1988. Critical two-phase flow through rough slits. Intern. J. Multiphase Flow 14 (2), 155–174.

Jones Jr, O.C., 1976. An improvement in the calculation of turbulent friction in rectangular ducts. J. Fluids Engng. 98, 173–181.

Körner, St., Friedel, L., 1998a. Ermittlung der Blasengeschwindigkeit einer Luft/Wasser-Strömung mit Hilfe der Hochgeschwindigkeitskinematographie. Forsch. Ingenieurwes 64 (1/2), 5–10.

Körner, St., Friedel, L., 1998b. Assessment of the maximum possible superheating of fluids during leakage flow. Chem. Eng. Technol. 21 (3), 267–271.

Körner, St., 1999. Theoretische und experimentelle Untersuchung der fluiddynamischen und thermodynamischen Ungleichgewichte bei der Zweiphasenströmung durch enge Spalte. Doctoral Dissertation, Techn. Univ., Hamburg-Harburg.

Leung, J.C., Grolmes, M.A., 1987. The discharge of two-phase flashing flow in a horizontal duct. AIChE J. 33 (3), 524–527.

Pana, P., 1975. Eine modifizierte Bernoulli-Gleichung für die Berechnung der Strömungsvorgänge im unterkühlten Wassergebiet. Wiss. Bericht, IRS-W-18.

Schrock, V.E., Revankar, S.T., Lee, Sy., Wang, C.-H., 1986. A computational model for critical flow through intergranular stress corrosion cracks. Report LBL-21967.

Westphal, F., 1991. Berechnungsmodell für die Leckraten aus Rissen in Wänden druckführender Apparate und Rohrleitungen. Doctoral Dissertation, University of Dortmund.

Westphal, F., Friedel, L., 1992. Mechanistic crack leakage rate prediction method. J. Heat Technol. 10 (1/2), 75–106.

Westphal, N., 1981. Keimverteilungsmessung mit dem Laser-Streulichtverfahren bei Tragflügel- und Propeller-Strömungen. Bericht Nr. 408 Institut für Schiffbau, University of Hamburg.